

MLBP



AFWAL-TR-86-4042

ADA178283

CRYSTALLIZATION AND MORPHOLOGY OF POLY (ARYL ETHER ETHER KETONE)

Satish Kumar
David P. Anderson
University of Dayton Research Institute
Dayton, Ohio 45469

W. W. Adams
Materials Laboratory
Wright Aeronautical Laboratories
Wright-Patterson AFB Ohio 45433-6533

December 1986

Interim Report for Period June 1983 - July 1985

Approved for Public Release; Distribution is Unlimited

Best Available Copy

MATERIALS LABORATORY
AIR FORCE WRIGHT AERONAUTICAL LABORATORIES
AIR FORCE SYSTEMS COMMAND
WRIGHT-PATTERSON AIR FORCE BASE, OHIO 45433-6533

20040219030

NOTICE

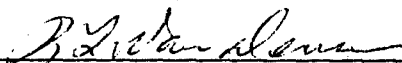
When Government drawings, specifications, or other data are used for any purpose other than in connection with a definitely related Government procurement operation, the United States Government thereby incurs no responsibility nor any obligation whatsoever; and the fact that the Government may have formulated, furnished, or in any way supplied the said drawings, specifications, or other data, is not to be regarded by implication or otherwise as in any manner licensing the holder or any other person or corporation, or conveying any rights or permission to manufacture use, or sell any patented invention that may in any way be related thereto.

This report has been reviewed by the Office of Public Affairs (ASD/PA) and is releasable to the National Technical Information Service (NTIS). At NTIS, it will be available to the general public, including foreign nationals.

This technical report has been reviewed and is approved for publication.

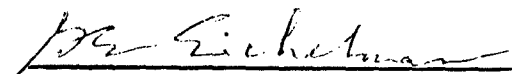


W. W. ADAMS
Project Scientist



R. L. VAN DEUSEN, Chief
Polymer Branch

FOR THE COMMANDER



GAIL E. EICHELMAN, Assistant Director
Nonmetallic Materials Division

"If your address has changed, if you wish to be removed from our mailing list, or if the addressee is no longer employed by your organization please notify AFWAL/MLBP, Wright-Patterson AFB OH 45433-6533 to help us maintain a current mailing list."

Copies of this report should not be returned unless return is required by security considerations, contractual obligations, or notice on a specific document.

REPORT DOCUMENTATION PAGE

1a. REPORT SECURITY CLASSIFICATION Unclassified			1b. RESTRICTIVE MARKINGS N/A			
2a. SECURITY CLASSIFICATION AUTHORITY			3. DISTRIBUTION/AVAILABILITY OF REPORT Approved for public release; distribution is unlimited			
2b. DECLASSIFICATION/DOWNGRADING SCHEDULE						
4. PERFORMING ORGANIZATION REPORT NUMBER(S) AFWAL-TR-86-4042			5. MONITORING ORGANIZATION REPORT NUMBER(S)			
6a. NAME OF PERFORMING ORGANIZATION Materials Laboratory		6b. OFFICE SYMBOL (If applicable) AFWAL/MLBP	7a. NAME OF MONITORING ORGANIZATION			
6c. ADDRESS (City, State and ZIP Code) Wright-Patterson AFB OH 45433-6533			7b. ADDRESS (City, State and ZIP Code)			
8a. NAME OF FUNDING/SPONSORING ORGANIZATION		8b. OFFICE SYMBOL (If applicable)	9. PROCUREMENT INSTRUMENT IDENTIFICATION NUMBER			
8c. ADDRESS (City, State and ZIP Code)			10. SOURCE OF FUNDING NOS.			
			PROGRAM ELEMENT NO.	PROJECT NO.	TASK NO.	WORK UNIT NO.
11. TITLE (Include Security Classification) <i>Crystallization & Morphology of Poly(Aryl Ether Ether Ketone)</i>			61102F	2303	Q3	07
12. PERSONAL AUTHOR(S) Satish Kumar, David P. Anderson, and W. Wade Adams						
13a. TYPE OF REPORT Interim		13b. TIME COVERED FROM <u>Jun 83</u> TO <u>Jul 85</u>	14. DATE OF REPORT (Yr., Mo., Day) 1986/December		15. PAGE COUNT 40	
16. SUPPLEMENTARY NOTATION						
17. COSATI CODES			18. SUBJECT TERMS (Continue on reverse if necessary and identify by block number)			
FIELD	GROUP	SUB. GR.				
07	04		PEEK Poly(aryl ether ether ketone) SALS			
11	04		Spherulite Birefringence SAXS WAXS			
19. ABSTRACT (Continue on reverse if necessary and identify by block number) The morphology of poly(aryl ether ether ketone) (PEEK) has been studied using optical microscopy (at room temperature and at elevated temperatures), small angle light scattering (Hv and Vv), transmission electron microscopy (bright field, dark field, and selected area electron diffraction), and wide and small angle x-ray scattering. As expected, density of nucleation and hence spherulite size depends on melt temperature. Higher melt temperatures gives rise to low nucleation density and hence large spherulites. The spherulite growth rate is independent of melt temperature and depends on crystallization temperature. The sign of the spherulite birefringence was determined between room temperature and 320°C by polarizing microscopy and at room temperature by Vv light scattering. In this temperature range the spherulites were negatively birefringent. From selected area electron diffraction, the crystal unit cell b-axis is found to align along the radius of the spherulite. The crystallographic (110) plane, which makes an angle of 52.7 degrees with the radial b-axis, appears to be the preferred growth plane. Chain polarizability was also calculated using refined atomic coordinates and the bond						
20. DISTRIBUTION/AVAILABILITY OF ABSTRACT UNCLASSIFIED/UNLIMITED <input checked="" type="checkbox"/> SAME AS RPT. <input type="checkbox"/> DTIC USERS <input type="checkbox"/>			21. ABSTRACT SECURITY CLASSIFICATION Unclassified			
22a. NAME OF RESPONSIBLE INDIVIDUAL W. W. Adams			22b. TELEPHONE NUMBER (Include Area Code) (513) 255-9148	22c. OFFICE SYMBOL AFWAL/MLBP		

11. Poly(aryl ether ether ketone)

19. polarizabilities. PEEK crystals were more stable in the electron beam, by about an order of magnitude, than polyethylene.

FOREWORD

This report was prepared by the Polymer Branch of the Nonmetallic Materials Division and The University of Dayton Research Institute (UDRI) under contract F33615-84-C-5020. The work was initiated under Project 2303, "Research to Define the Structure Property Relationships," Task 2303Q3, Work Unit Directive 2303Q307, "Structural Resins." Dr. Thaddeus E. Helminiak served as the AFWAL/ML Work Unit Scientist. Co-authors were: Satish Kumar and David P. Anderson (UDRI) and W. W. Adams (AFWAL/MLBP).

The atomic coordinates in the repeat unit were made available by Professor A. V. Fratini and the computer program for the calculation of chain polarizabilities was written by Dr. P. T. Bapu of the University of Dayton. The authors are grateful for useful comments on the manuscript from Professor E. L. Thomas of the University of Massachusetts.

This report covers research conducted from June 1983 to July 1985.

1. INTRODUCTION

Poly(aryl ether ether ketone) (PEEK), repeat unit shown in figure 1a*, crystallizes into an orthorhombic unit cell structure (ref. 1-3). The synthesis of this family of polymers is described by Attwood et al. (ref. 4). Crystallization behavior and spherulitic growth have been studied by Blundell and Osborn (ref. 5), and PEEK was shown to behave much in the same way as poly(ethylene terephthalate). The morphology and solution properties of PEEK have been the subject of recent studies (ref. 6-8).

The orthorhombic unit cell of PEEK has values of \underline{a} , \underline{b} , and \underline{c} which are reported to be in the range of 7.75-7.78 Å, 5.89-5.92 Å, and 9.88-10.06 Å respectively. The unit cell contains two chains each with two-thirds of the repeat unit. However a unit cell with two repeat units has recently been considered (ref. 9). The crystal structure of PEEK is similar to the reported (ref. 10) crystal structure of poly(p-phenylene oxide), and the ether and carbonyl units are considered to be crystallographically equivalent (ref. 3). The crystal structure is shown in figure 1b.

PEEK is a candidate as a thermoplastic to be used in composites (ref. 11), the properties of which will depend on processing history and morphology. Therefore the understanding of morphology and its dependence on processing parameters is important. We have studied the crystallization behavior of PEEK from the melt in a polarizing microscope. The morphology of PEEK spherulites has been studied using light-scattering and x-ray-scattering, optical microscopy, as well as transmission electron microscopy (dark field, bright field, and selected area electron diffraction). The results of these investigations are reported herein.

*Figures and tables are located at end of report.

2. EXPERIMENTAL METHODS

Studies reported in this paper were conducted on commercially available PEEK received from Imperial Chemical Industries.

Crystallization studies were done in a metallurgical hot stage on a Leitz optical microscope. A very small amount of PEEK resin (few milligrams) is sandwiched between two circular glass plates of about half-a-centimeter in diameter. The hot stage is then heated to the desired melt temperature (between 380 C and 420 C) above the melting point of PEEK which is reported to be in the range of 335 C to 350 C. After 5 minutes at the melt temperature the hot stage is set to the crystallization temperature (300 C or 320 C) and the hot stage containing the specimen reaches this temperature in approximately 30 seconds. Spherulite growth was recorded at the crystallization temperature as a function of time, using crossed polars, on Kodak VR1000 35 mm film.

Wide-angle x-ray-scattering (WAXS), transmission electron microscopy (TEM), and small-angle x-ray-scattering (SAXS) were performed on the samples prepared in the following way. A mold containing the resin was placed in a compression molding press preheated to 400 C, and nominal pressure was applied. A thermocouple was in contact with the resin. In one case, 5 minutes after the thermocouple reached 400 C the press heaters were turned off. The specimen reached room temperature in about 3 hours. This specimen is referred to as slow-cooled (SC). In another case, 5 minutes after the thermocouple reached 400 C, the mold containing the resin was removed from the hot press and kept in a second press which was at room temperature. This specimen came to room temperature in a few minutes and is referred to as fast-cooled (FC). Similar samples were also made from 420 C.

WAXS was done using the symmetric transmission geometry on a four-circle automated Picker diffractometer. Lorentz, polarization, Compton-scattering, and absorption corrections were applied. Correction for instrumental line broadening for the crystal size measurement was done using crystalline hexamethylenetetramine. For TEM, thin sections were prepared by using a diamond knife to ultramicrotome epoxy-embedded blocks of PEEK at room temperature. Transmission electron microscopy was done on a JEOL 100CX at 100 KV. SAXS was done on a modified Statton (Warhus) camera with pin-hole collimation, camera-to-film distance of 72cm, and CuK α radiation. No corrections were applied to the SAXS data.

3. RESULTS AND DISCUSSION

3.1 Nucleation and growth

Isothermal crystallization of PEEK at 320 C, from the melt at 380 C and at 420 C, is shown in figures 2 and 3 respectively. In figure 2 only the completion of spherulite growth is shown. This is because nucleation density was high in the specimens crystallized from lower melt temperatures, therefore spherulites growth is shown. This is because nucleation density was high in the specimens crystallized from lower melt temperatures, therefore spherulites filled the volume rather quickly and spherulitic growth could not be monitored visually. However, such growth can be monitored with a state-of-the-art, automated small-angle light-scattering apparatus (ref. 12). Figure 3 shows crystallization from higher melt temperature, with lower nucleation density.

Spherulitic growth rate was monitored at crystallization temperatures of 300 C and 320 C from a melt of 420 C by measuring the spherulite radii from

optical micrographs taken at successive intervals. The radius can also be calculated from small-angle light-scattering (Hv) using the following equation

$$4\pi(R_s/\lambda) \sin(\theta_{\max}/2) = 4.1 \quad (1)$$

where θ_{\max} is the angle at maximum intensity, λ is the wavelength of light, and R_s is the radius of the spherulite. For two-dimensional spherulites (ref. 13) the constant in equation 1 will be 3.8 instead of 4.1. Typical Hv and Vv light-scattering patterns of PEEK at room temperature are given in figure 4. Spherulite sizes from optical micrographs and from SALS were identical within the limits of experimental error. Average spherulite radius, measured from optical micrographs up to the point where they start impinging on each other, has been plotted in figure 5 for a crystallization temperature of 320 C. The growth is linear and the average growth rates were 0.045 m/sec at 320 C and 0.32 m/sec at 300 C. Blundell and Osborn have reported the maximum crystallization rate to be around 230 C as studied from differential scanning calorimetry, with some dependence on heating rate. Qualitatively our spherulite growth data is in agreement with this observation in that we observe a higher growth rate at 300 C than at 320 C. However, quantitatively the growth rate observed by us at 300 C corresponds to that between 260 C and 270 C by Blundell and Osborn (the values of G in table 3 of reference 5), and extrapolation of their data to 300 C would give a lower growth rate than what we have observed. This may occur for several reasons: (i) differences in molecular weight, (ii) secondary crystallization which will be observed in DSC but not in optical micrographs; and

(iii) Blundell and Osborn calculated growth rate assuming that the peak crystallization time, t_c , corresponds to the point where the spherulites impinge. Peak crystallization time would be analogous to the crystallization time for figure 3(c) of this paper, which is an overestimation, because the majority of the spherulites have stopped growing much earlier (figure 3(b).)

A plot of the logarithm of nucleation density (number of spherulites per unit volume) as a function of melt temperature is given in figure 6. Within the temperature range of the experiment nucleation density seems to fall off exponentially with the temperature increase (logarithm of nucleation density as a function of temperature is linear within the limits of experimental error). Observation of the change in nucleation density in PEEK, as a function of the temperature to which the melt was heated and the dwell time at the high temperature, is by no means unique and has been reported for a number of polymers (ref. 14). Possible reasons for the change in nucleation density as a function of the melt temperature are discussed below:

(i). The melting point of PEEK has been reported to be 335 C (ref. 4, 5) and 350 C (ref. 15). However, the thermodynamic melting temperature, at which perfect crystals of infinite size melt, has been estimated (ref. 4) to be 395 C. This leads to the possibility of the presence of some unmelted crystals at a temperature higher than the normally measured melting point.

Self-nucleation by residual high molecular weight crystals can also possible account for the above observation (ref. 14). The degree of self-nucleation (number of embryos) decreases with increasing temperature, and hence results in larger spherulite size from higher melt temperatures.

(ii). Impurities in the specimen can lead to nucleation. A decrease in nucleation density has been observed in purifying the material (ref. 7). The purification was done by dissolving the material in sulfuric acid and reprecipitating it. The problem of sulfonation of PEEK during treatment in sulfuric acid also remains. In addition to the impurities which were removed in acid the possibility of the presence of some other species of the poly(aryl-ether-ketone) family (one of the species is reported (ref. 4) to have a melting point of 416 C) cannot be excluded as a result of impurities in the starting materials used in the synthesis. Since ether and ketone units are crystallographically equivalent (ref. 3) certain different species of the poly(aryl-ether-ketone) family may be able to crystallize together. One nucleating crystal in one hundred billion crystals of average dimension of 100 Å, in a 50-percent-crystalline medium, will produce an average spherulite radius of 36 μm.

Since the melting and crystallization studies reported in this paper are done at rather high temperatures, it is only natural that the effect of these conditions on polymer degradation be considered. The large spherulite size has in fact been attributed to degradation from high melt temperatures (ref. 7). Therefore the effect of air at high temperatures must be considered. Viscosity measurements (ref. 16) on PEEK in the presence of air in the temperature range of 350 C to 380 C, showed an increase in viscosity with increasing dwell time, which was attributed to crosslinking. Chain extension may also be a possible cause for viscosity increase, but this is likely to be very limited because of the restricted mobility of the reactive groups. Degradation will result in a decrease in viscosity. Chain crosslinking or

chain extension would only result in inhibiting crystallization. In our optical microscope studies the specimen has been heated between two glass plates with virtually no air gap. Melting and recrystallization over several cycles, melt time held to five minutes, resulted in reproducible spherulite size and growth rate although nucleation did not occur in the same positions after each melting. Also the PEEK resin between the microscope slides did not discolor on repeated melting except at the very edge. Therefore we believe that for this study significant degradation did not occur.

3.2 Birefringence

The sign of the spherulite birefringence can be determined using a polarizing microscope or from Vv light-scattering (ref. 13). A Vv light-scattering pattern of a PEEK sample, whose volume is completely filled with spherulites as observed in the polarizing microscope at room temperature, is given in figure 4b. This scattering pattern is strongly oriented along the polarization direction indicating that the difference between the radial and tangential polarizabilities is greater than the difference between either one of them and the effective polarizability of the surroundings of the spherulite. The surroundings of the spherulite consists of other spherulites since the whole volume is filled with them, and hence the polarizability of the surroundings will be the average of the radial and tangential polarizability. From this one can conclude that tangential polarizability is larger than the radial polarizability.

The spherulite birefringence sign was also determined, from room temperature to 320 C, using a polarizing microscope and a wave

plate (ref. 17). In the entire temperature range the spherulites were found to be negatively birefringent. The absolute value of birefringence was estimated using a Leitz tilting compensator to be approximately -0.02. The observation of negatively birefringent spherulites in PEEK is contrary to the previously published observation (ref. 5) in which PEEK spherulites were positively birefringent. Since the spherulite of the same material can be negatively or positively birefringent, depending upon crystallization conditions, this difference in the birefringence sign between our and the previously published observation (ref. 5) needs further investigation.

The chain anisotropy can be calculated using the bond polarizabilities and the angles between different bonds (ref. 18-20). Chain polarizability in three different directions is given by the following equations:

$$\alpha_a = \Sigma \left[(\alpha_1 - \alpha_2) \sin^2 \theta \cos^2 \phi + \alpha_2 \right] \quad (2)$$

$$\alpha_b = \Sigma \left[(\alpha_1 - \alpha_2) \sin^2 \theta \sin^2 \phi + \alpha_2 \right] \quad (3)$$

$$\alpha_c = \Sigma \left[(\alpha_1 - \alpha_2) \cos^2 \theta + \alpha_2 \right] \quad (4)$$

where the summation is over the whole repeat unit, θ is the angle which the bond makes with the c-axis, and ϕ is the angle which the projection

of the bond on the a-b plane makes with the a-axis. α_1 and α_2 are the bond polarizabilities parallel and perpendicular to the bond respectively. The bond polarizability values are listed in table 1.

The PEEK chain coordinates have been refined in our laboratory (ref. 21). Using these refined coordinates the following values of polarizabilities were calculated.

$$\alpha_{\underline{a}} = 3.38 \times 10^{-23} \text{ cm}^3.$$

$$\alpha_{\underline{b}} = 2.31 \times 10^{-23} \text{ cm}^3.$$

$$\alpha_{\underline{c}} = 4.02 \times 10^{-23} \text{ cm}^3.$$

Polarizability of the chain and its refractive index, n , are related by the Lorenz-Lorentz equation:

$$\frac{(\eta^2 - 1)M}{(\eta^2 + 2)d} = \frac{4\pi}{3} \alpha N \quad (5)$$

where N is Avogadro's number, d is the bulk density of the material, and M is the molecular weight of the repeat unit. Using a PEEK crystalline density (ref. 5) of 1.40 gram/cm^3 and the above values of chain polarizabilities in three different directions, $n_{\underline{a}}$, $n_{\underline{b}}$, and $n_{\underline{c}}$ were calculated to be 1.77, 1.48, and 1.97 respectively. Birefringence calculated using equation 5 is generally not in agreement with the observed value, and this is attributed to the presence of internal field effects. However birefringence in the

spherulite and in a fiber was calculated using the above refractive indices. As will be noted in a later section, the b crystal axis is radial in the PEEK spherulite. Therefore the birefringence in the spherulite will be given by $n_{\underline{b}} - ((n_{\underline{a}} + n_{\underline{c}})/2)$, or $n_{\text{spherulite}} = -0.39$, which is about twenty times larger than the observed value. Such a difference in the observed and calculated birefringence has been attributed to imperfect crystalline orientation, the presence of amorphous regions, and form birefringence (ref. 13).

The birefringence in the fiber will be given by $n_{\underline{c}} - ((n_{\underline{a}} + n_{\underline{b}})/2)$ and for the above refractive indices its value is 0.34. Experimental measurement of birefringence on highly oriented PEEK fibers gave birefringence values of up to 0.28. Because of the presence of less than perfect orientation in the fiber and the presence of amorphous regions, the true birefringence of the PEEK fiber would be higher than 0.28. This indicates that the calculated birefringence of PEEK fiber may be close to the true value.

3.3 Crystallinity and Long Period

Crystallinity was determined from wide angle x-ray scattering (WAXS) using Ruland's method (ref. 22-24). The main features of this method can be described by the following equations:

$$R(s_p^2) = \frac{\int_{s_o}^{s_p} s^2 I ds}{\int_{s_o}^{s_p} s^2 I_{cr} ds} \quad (6)$$

$$R(s_p^2) = I/X_{cr} + (k/2X_{cr}) \cdot s_p^2 \quad (7)$$

where s is $2\sin\theta/\lambda$, and θ is half the scattering angle and λ the wavelength of radiation used. s_o and s_p represent the lower and upper limits of the scattering range. I and I_{cr} are the total and crystalline intensities respectively. X_{cr} is the degree of crystallinity and k is the disorder parameter. A typical plot of s^2I versus s is given in figure 7. An amorphous PEEK diffraction scan was fit to the intensities between crystalline peaks (25), which is also shown in the shaded areas in figure 7. From this curve $R(s_p^2)$ was calculated for different values of s_p^2 . A plot of $R(s_p^2)$ as a function of s_p^2 is given in figure 8, which is approximately a straight line. From the slope and intercept of this line the values of crystallinity and disorder parameters were obtained using equation 7.

Parameters obtained from WAXS and SAXS are listed in table 2 for resin samples slow cooled from 400 and 420 C, and fast-cooled from 400 C. From this table it is noted that, as expected, the fast-cooled sample has both lower crystallinity and higher crystalline disorder compared to a slow-cooled sample from the same melt temperature. For slow cooled samples, crystallization from a higher melt temperature gives rise to a slightly lower value of crystallinity and higher crystalline disorder. The crystallinity values of 36% to 43% are in the upper range of the reported (ref. 5) PEEK crystallinity values (0% to 45%). However, it must be noted that the crystallinity as determined by Ruland's method (ref. 22) generally gives higher values than obtained from simple intensity ratios since the values from Ruland's method includes disorder effects.

Approximate crystallite sizes were determined from the line breadth of the (211) reflection by Wilson's variance method (ref. 26,27). The

contribution to the line breadth from disorder was ignored, and hence the crystal size reported in this paper represents the lower bound. The (211) reflection was chosen because it did not overlap other reflections. The size calculated for the sample slow-cooled from 420 C was larger than the size calculated for the sample cooled from 400 C despite the higher disorder in the sample from the higher temperature which would tend to decrease the calculated size. The fast-cooled sample shows an even smaller crystallite size. Approximate crystallite sizes were also calculated from the line-broadening of the (110) and (200) reflections, which in turn were obtained by curve-fitting the data. In the case of the (110) and (200) reflection the subtraction of the instrumental line broadening was done assuming gaussian profiles (the observed broadening is the sum of the squares of the specimen and instrumental broadening). The instrumental line profile was indeed gaussian, however the specimen profiles were best fitted with a Pearson-type VII function. Again the sample slow-cooled from 420 C shows larger crystallite sizes than the other two samples. In this analysis no significant differences between the fast and slow-cooled samples from 400 C can be detected.

The unit cell parameters calculated from the positions of the reflections obtained during the curve-fitting operation are also reported in table 2. From these values it is noted that the fast-cooled sample has larger values of a and c axes compared to the slow-cooled sample is perhaps due to the chain-packing disorder in the a and c axes directions.

While several differences were observed in the WAXD analysis, a greater range of process conditions will have to be investigated to fully understand the crystalline behavior of this material.

3.4 Electron Radiation Damage

Different polymers are damaged in the electron beam to varying degrees (ref. 28-31). In order to obtain useful information on the morphology of polymers using electron microscopy, it is important that the polymer not be exposed to such levels of electron radiation dose that the features of interest are destroyed or altered significantly. A systematic study was therefore undertaken (ref. 31) to quantitatively determine the dose required to damage different polymers to the point where the intensity of diffraction is reduced by a factor of $1/e$. This dose level is generally termed as D^* and its value for several polymers has previously been reported (ref. 28). The D^* value(31) for the (110) reflection of PEEK, at a dose rate of 10^{-3} amp/cm² is approximately 3×10^{-2} Coulomb/cm². This is about an order of magnitude greater than the D^* value for polyethylene. The higher resistance of PEEK in the electron beam makes it relatively easier to study in the electron microscope.

3.5 Radial and Growth Direction

Figure 9 shows an electron micrograph from a thin section microtomed from a specimen fast-cooled from the melt at 400 C. In this figure, as observed from selected area electron diffraction, regions marked A were amorphous and regions marked B were semicrystalline. The chatter produced due to microtoming is largely responsible for contrast in the A regions. The B regions are spherulites, which could not grow further due to fast-cooling.

In this specimen it was observed that a fraction of spherulites have grown to their fullest extent. From this it can be inferred that for complete crystallization from higher melt temperatures relatively slow-cooling rates would be required. In the fast cooled sample row nucleation was also observed as shown in figure 10. Such nucleation has also been observed in isotactic polypropylene (ref. 32).

Transmission electron micrographs of a section of a spherulite in two different directions in a sample slow-cooled from the melt at 400 C are shown in figures 11a and b. From photographs taken on a large number of sections it was ascertained that the section in figure 11a is a diametrical section and the radial direction is in the plans of the paper. Selected area electron diffraction patterns taken from different regions are shown in figures 11a and 11b; the corresponding regions are indicated by black arrows. The two diffraction patterns in figure 11a are similar except that the diffraction pattern from the center of the spherulite is less oriented as expected. The (110) reflection is the strongest in figure 11(a) and is missing in figure 11(b). From the orientation of the diffraction pattern in figure 11a it can be seen that the crystal unit cell b-axis is radial and hence the a and c axes are tangential.

The growth direction of a spherulite is along its radius, and therefore one would expect that the preferred growth plane in PEEK spherulites would be an (010) plane. Information regarding the preferred growth plane can be obtained from dark field electron microscopy. A dark field electron micrograph using the (110) reflection is shown in figure 12. Careful examination of the dark field electron micrographs (see the circled region in

figure 12) reveals that the growth faces of the crystallites and the radial direction of the spherulite are not perpendicular to each other. From a large number of these crystals where the growth face was distinct, the angle between the radial direction and growth face was measured to be 55 ± 8 degrees. The calculated angle between the \underline{b} axis and (110) plane is 52.7 degrees. This observation is suggestive of the fact that (110) is probably the preferred crystal growth plane. Following the dictates of the Bravais-Friedel law (ref. 33) the (110) plane was in fact assumed (ref. 5) to be the preferred growth plane in PEEK. Reported work on PEEK single crystals (ref. 6) also suggests (110) as the preferred growth plane.

One of the problems which one encounters in the electron microscopy of ultramicrotomed sections of polymers is the deformation introduced in the process of microtoming. Since we were using dark field micrographs obtained on ultramicrotomed sections to determine the preferred growth plane, the consideration of crystal orientation smearing due to ultramicrotoming was particularly important. Selected area electron diffraction on a large number of spherulites with different cutting directions indicated that the \underline{b} crystal axis was always radial and was independent of microtoming direction suggesting that no significant orientation smearing took place.

CONCLUSIONS

Crystallization of PEEK from the melt is sensitive to the melt temperature, with significant differences observed in the nucleation density, but only small differences in other parameters such as degree of crystallinity, crystallite size, disorder, and long period. Samples crystallized from higher melt temperature have a larger disorder parameter

and larger crystals. The nucleation density decreases with higher melt temperature, thereby resulting in larger spherulites. Spherulite growth was faster at 300 C compared to the growth rate at 320 C. PEEK crystallized from the melt was found to have negatively birefringent spherulites. However, since spherulites of the same material can be positive or negatively birefringent and since positively birefringent spherulites in PEEK have previously been reported, this aspect needs further work in order to resolve the question that there indeed are two different types of spherulites in PEEK. Calculated refracted index of PEEK crystals along the three crystallographic axes a, b, and c are respectively 1.77, 1.48, and 1.97. The b crystal axis is radial in the spherulites, and the crystals appear to have (110) as the preferred growth plane.

REFERENCES

1. P. C. Dawson and D. J. Blundell, *Polymer*, 21, 577 (1980).
2. D. R. Rueda, F. Ania, A. Richardson, I. M. Ward, and P. J. B. Calleja, *Polymer Communications*, 24, 258 (1983).
3. J. N. Hay, D. J. Kemmish, J. I. Langford, and A. I. M. Rae, *Polymer*, 25, 175 (1984).
4. T. E. Attwood, P. C. Dawson, J. L. Freeman, L. R. J. Hoy, J. B. Rose, and P. A. Staniland, *Polymer*, 22, 1096 (1981).
5. D. J. Blundell and B. N. Osborn, *Polymer*, 24, 953 (1983).
6. A. J. Lovinger and D. D. Davis, *Bulletin of the American Physical Society*, 30, 249 (March 1985), and the presentation in March APS meeting.
7. P. Cebe, S. D. Hong, S. Y. Chung, A. Gupta, and A. Yavourian in *Bulletin of the American Physical Society*, 30, pages 248, 488, 497 (March 1985).
8. M. T. Bishop, F. E. Karasz, P. S. Russo, and K. H. Langley, *Macromolecules*, 18, 86 (1985).
9. N. T. Wakelyn, *Polymer Communications*, 25, 207 (1984).
10. J. Boon and E. P. Magre, *Die Makromolekulare Chemie*, 126, 130 (1969).
11. J. T. Hartness and R. Y. Kim, 29th National SAMPE Symposium, 29, 459 and 765 (1984).
12. R. J. Tabar, R. S. Stein, and M. Long, *J. Polym. Sci. (Phys.)*, 20, 2041 (1982).
13. R. S. Stein and M. B. Rhodes, *J. Applied Physics*, 31, 1873 (1960); American Physical Society short course on "Scattering Methods in Polymer Science," at Chicago (March 1979), coordinated by R. S. Stein.
14. B. Wunderlich, "Macromolecular Physics, Vol II - Crystal Nucleation, Growth, Annealing," Academic Press, p. 52 (1976), and references cited on page 53.
15. R. N. Johnson, A. G. Fahrnam, R. A. Clendinning, W. P. Hale, and C. F. Merrian, *J. Polymer Sci. (Chem. ed.)*, 5, 2375 (1967).
16. Interim technical report no. 3 from Boeing Co. to AFWAL/MLBC on Thermoplastic Composite Technology Development, p. 16-18, May 1984.
17. E. M. Chamot and C. W. Mason, "Handbook of Chemical Microscopy," Vol I, John Wiley & Sons, p. 300 (1958).

18. C. W. Bunn, *Chemical Crystallography*, Oxford, London, 312 (1961).
19. J. Furukawa, S. Yamashita, T. Kotani, and M. Kawashima, *J. Appl. Polymer Sci.*, 13, 2527 (1969).
20. E. J. Roche, R. S. Stein, and E. L. Thomas, *J. Polymer Sci. (Phys ed.)*, 18, 1145 (1980).
21. A. Fratini, E. Cross, R. Whitaker, and W. W. Adams. Submitted to *Polymer*.
22. W. Rudland, *Acta Crystallographica*, 14, 1180 (1961).
23. C. G. Vonk, *J. Appl. Crystallography*, 6, 148 (1973).
24. D. P. Anderson, AFWAL-TR-85-4079, WPAFB, Ohio, 1985.
25. M. M. Hall Jr., V. G. Veeraraghavan, H. Rubin, and P. G. Winchell, *J. Appl. Cryst.*, 10, 66 (1977).
26. A. J. C. Wilson, *Proc. Physical Soc., London* 80, 286 (1962).
27. E. Pitts and F. W. Willets, *Acta Cryst.*, 14, 1302 (1961).
28. J. R. Minter, Ph.D. Thesis, *Polymer Sci. and Engr.*, University of Massachusetts, Amherst, p. 104 (1982).
29. E. L. Thomas and D. G. Ast, *Polymer*, 15, 37 (1974).
30. D. T. Grubb and G. W. Groves, *Phil. Mag.*, 24, 815 (1971).
31. S. Kumar, S. J. Krause, W. W. Adams, *Proceedings of Electron Microscopy Society of America*, 43, 84 (1985).
32. B. Maxwell, *J. Polymer Sci.*, C9, 43 (1965).
33. B. Wunderlich, "Macromolecular Physics, Vol I - Crystal Structure, Morphology, Defects," Academic Press (1973).

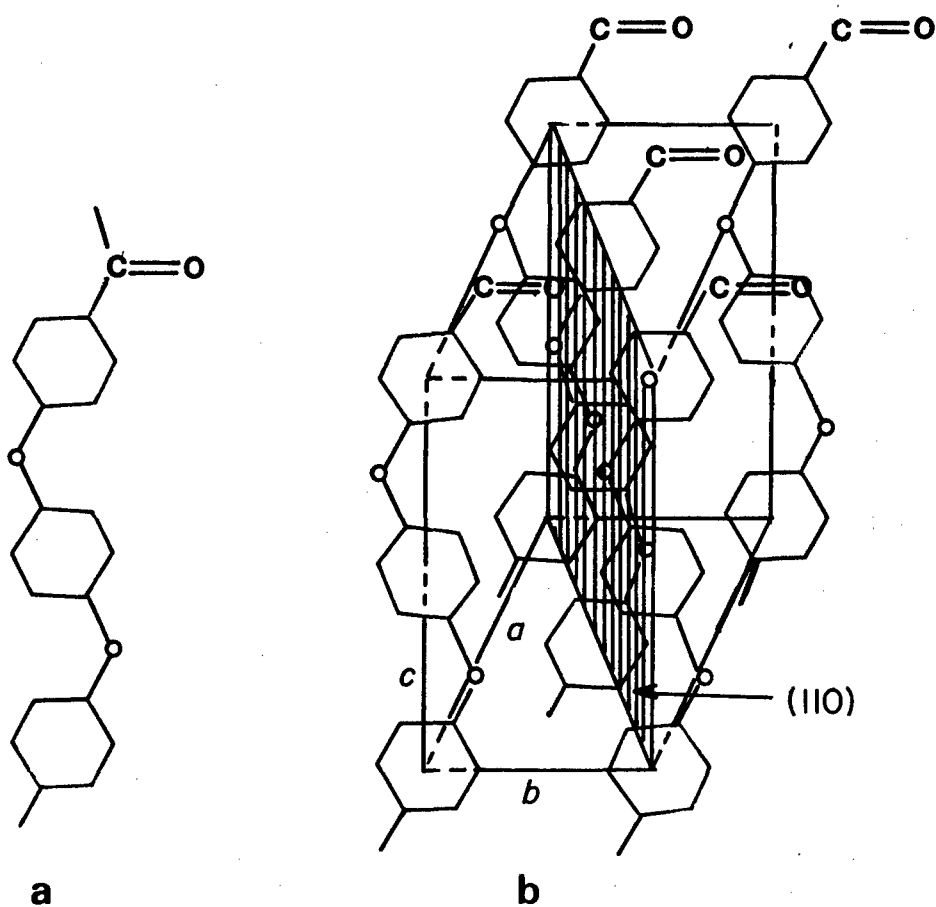


Figure 1.(a) Repeat unit of poly(aryl ether ether ketone);
 (b) Unit cell of PEEK (*c*-axis is shown from the center of the first phenyl ring to the center of the third phenyl ring).

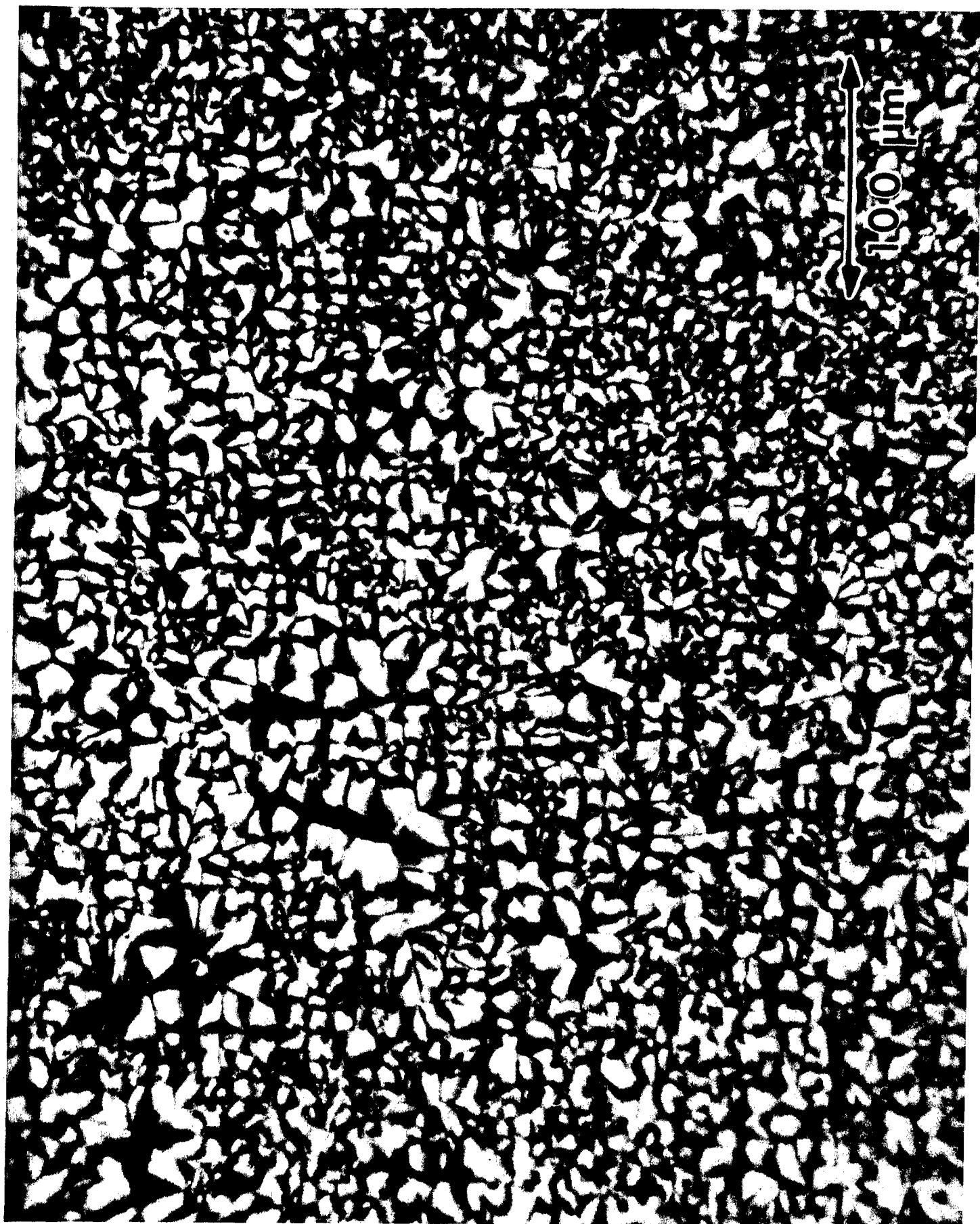


Figure 2. PEEK spherulites between cross polars at crystallization temperature (300°C). Melt conditions - 5 minutes at 380°C .

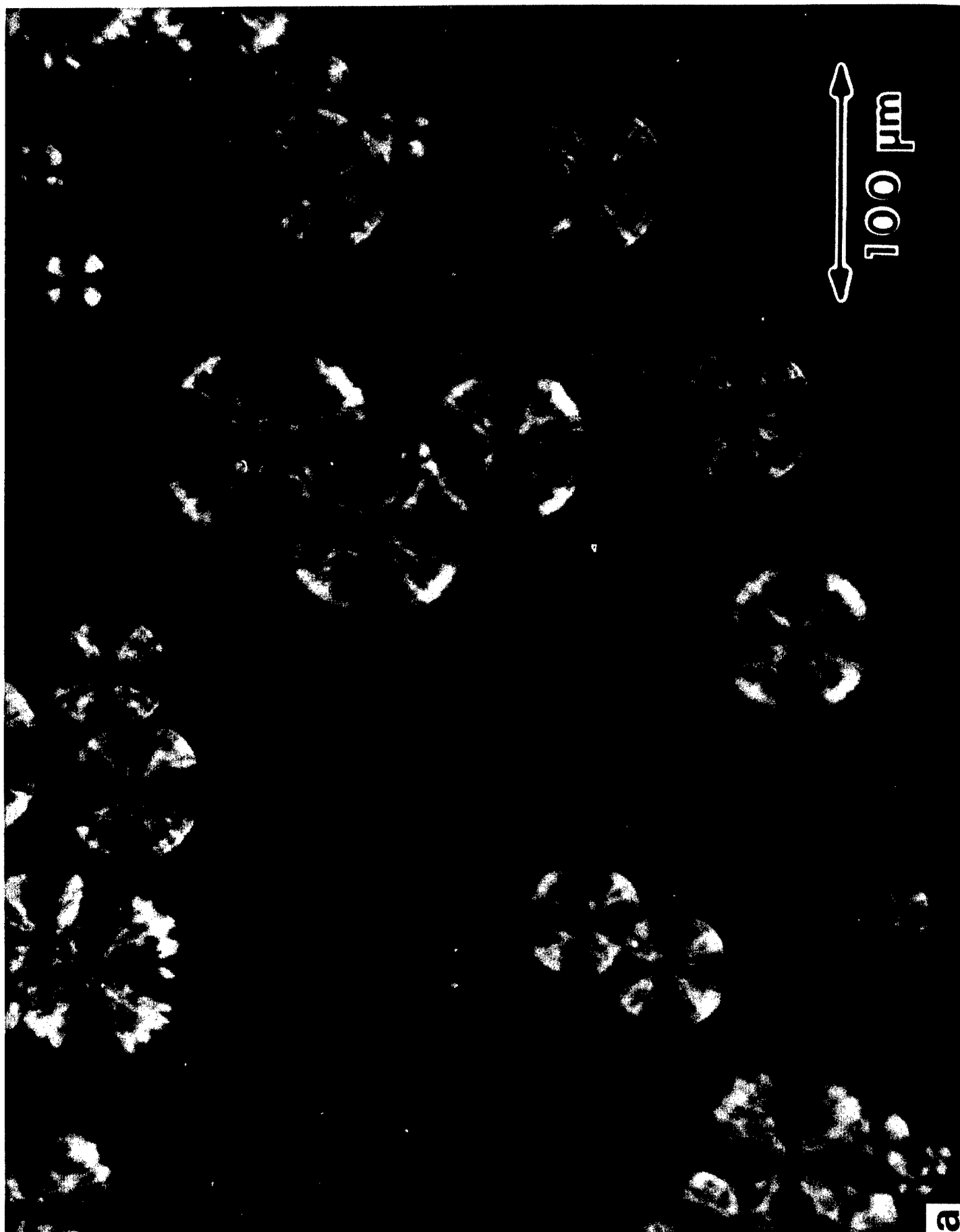


Figure 3.(a) Growth of PEEK spherulites, melt conditions - 5 minutes at 420°C crystallization temperature 320°C. Photographs taken at 320°C between crossed polars after 8 minutes.

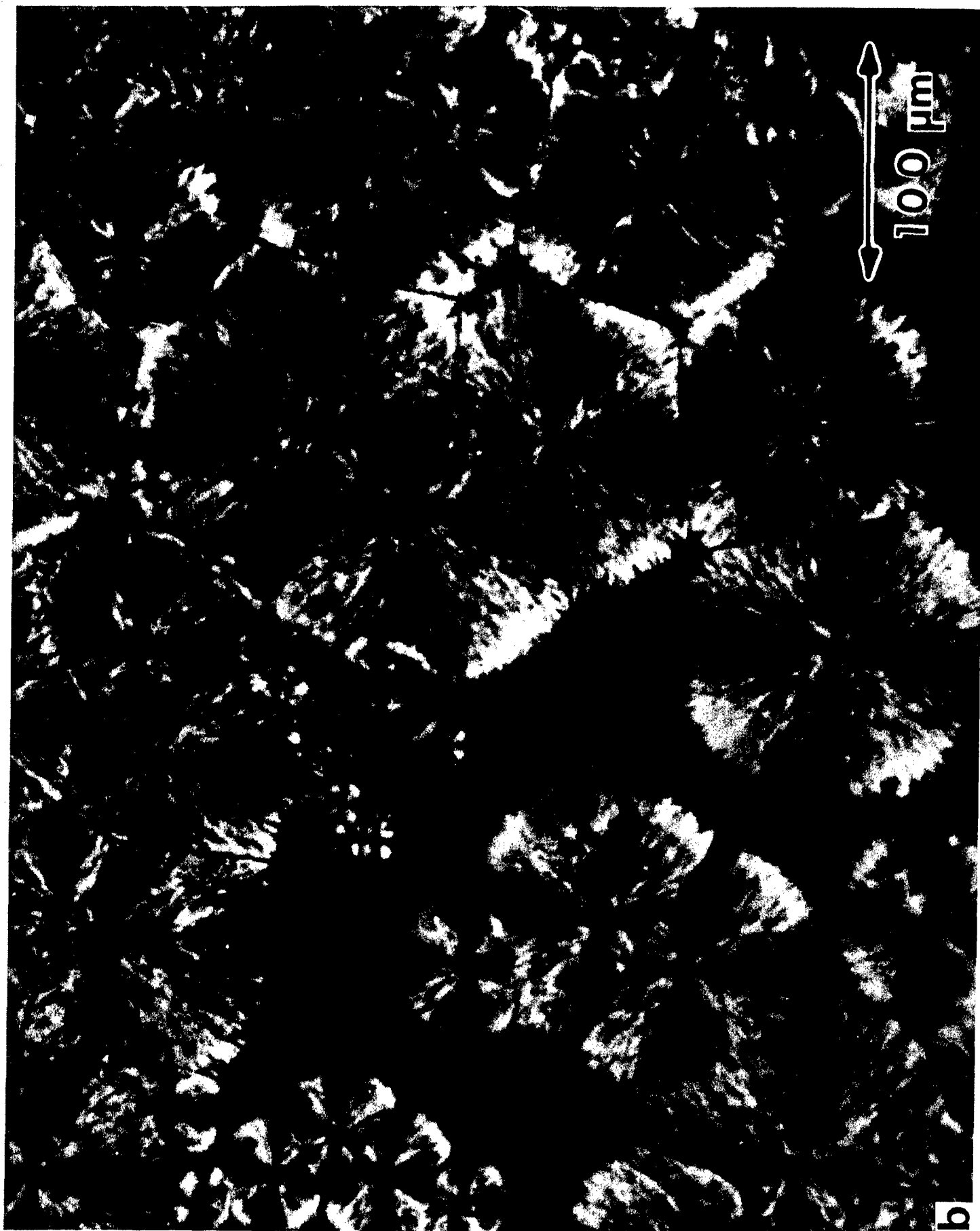


Figure 3.(b) Growth of PEEK spherulites, melt conditions - 5 minutes at 420°C , crystallization temperature 320°C . Photographs taken at 320°C between crossed polars after 16 minutes.

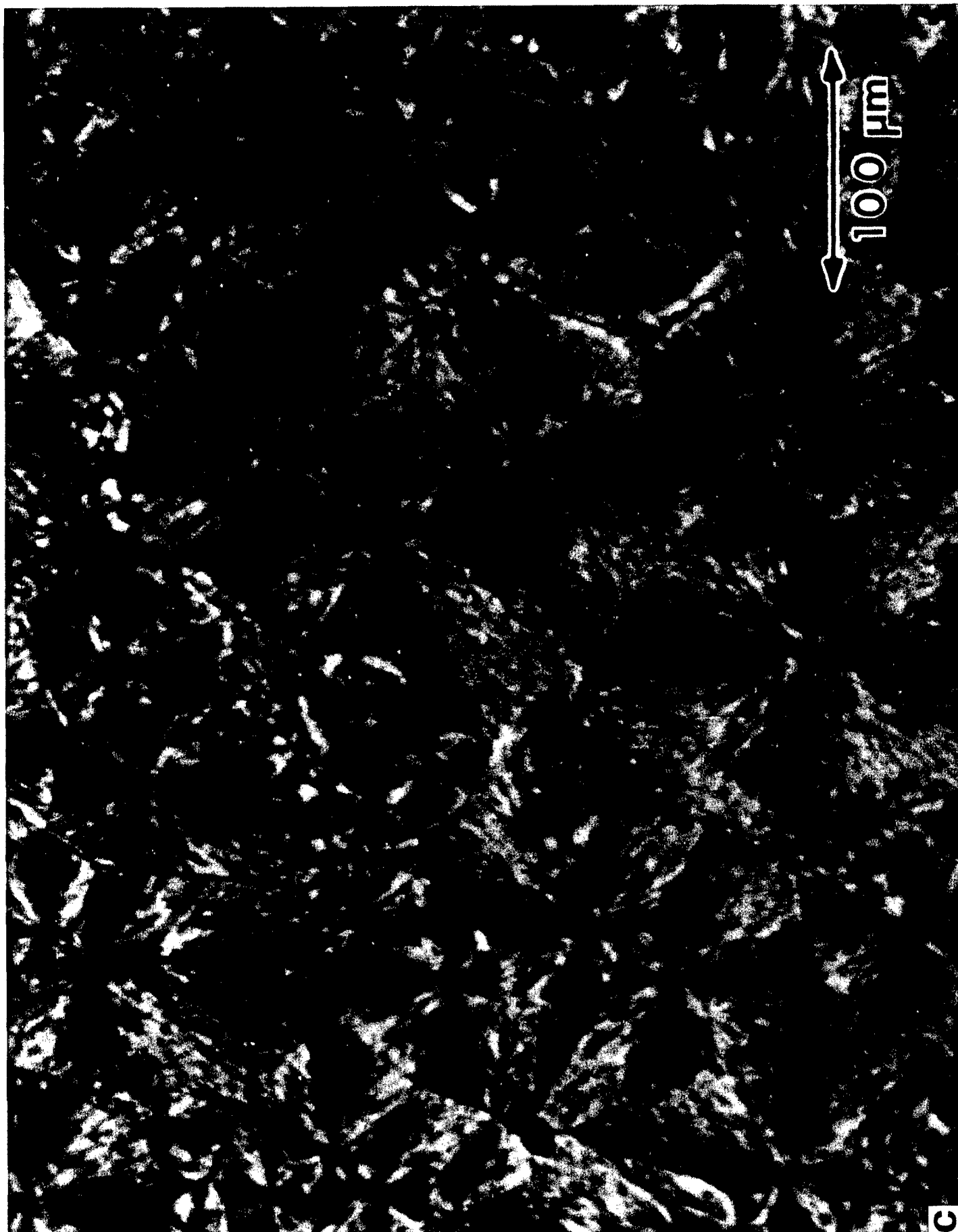


Figure 3.(c) Growth of PEEK spherulites, melt conditions - 5 minutes at 420°C , crystallization temperature 320°C . Photographs taken at 320°C between crossed polars after 24 minutes.

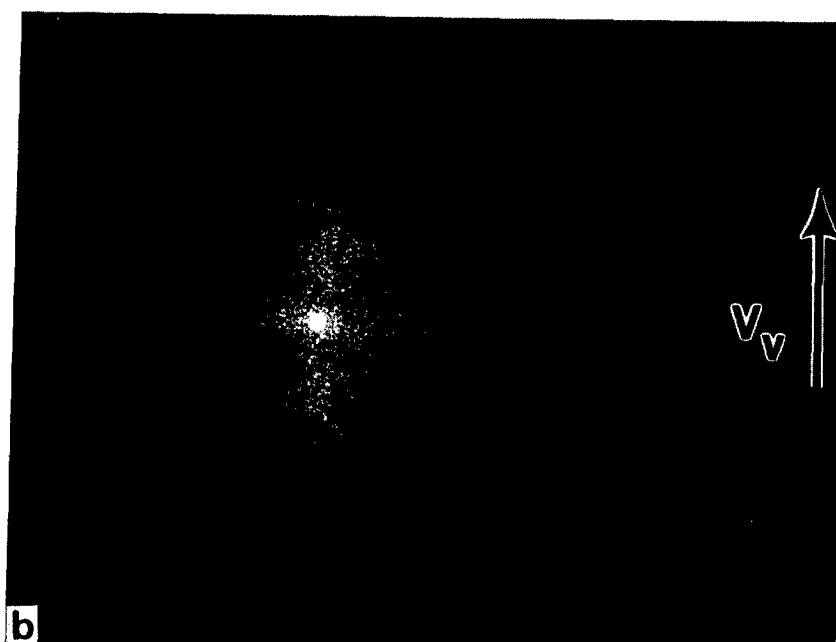


Figure 4.(a) Hv, and (b) Vv light scattering patterns of PEEK crystallized from melt at 420°C.

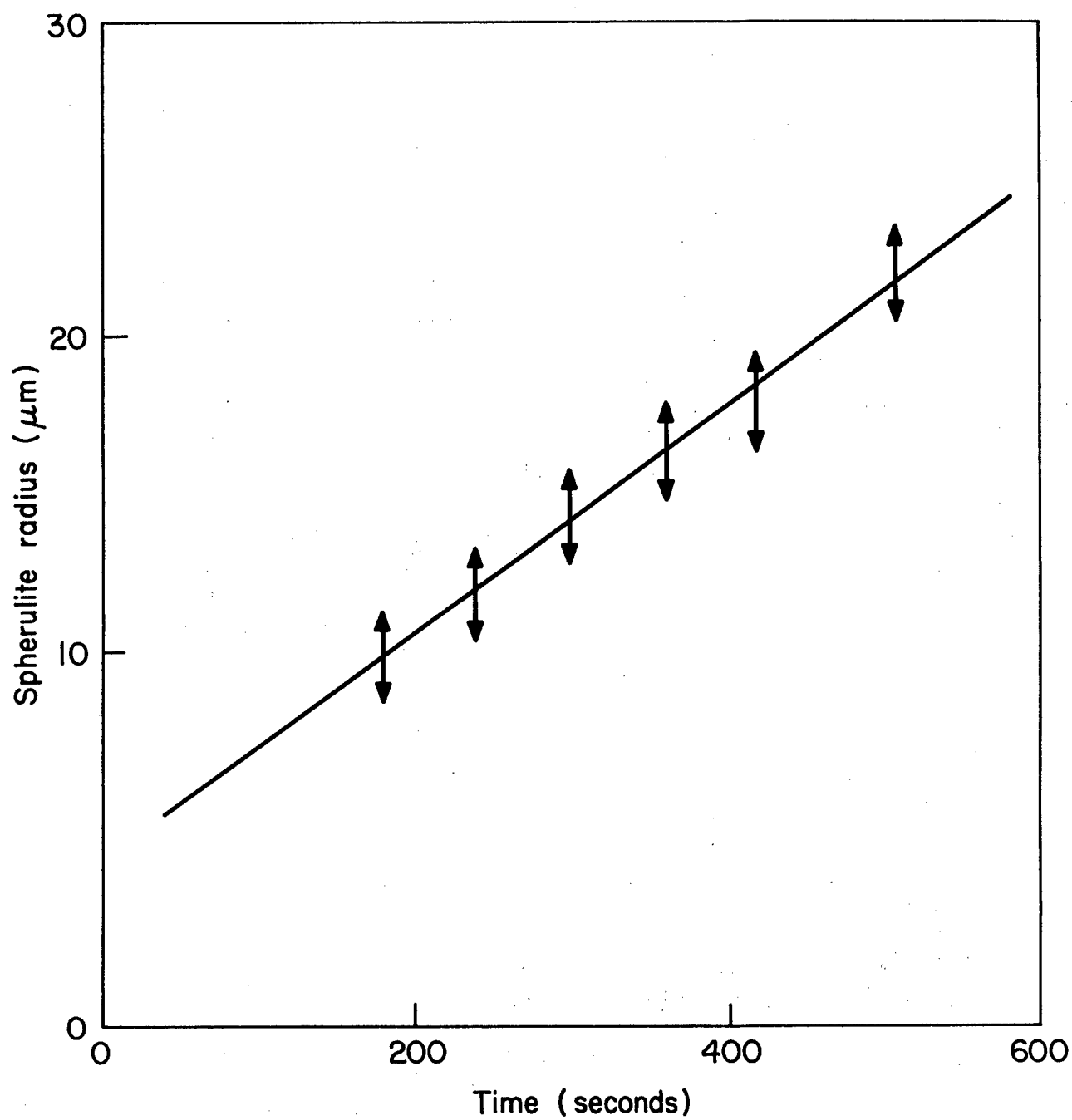


Figure 5. Linear isothermal radial growth of PEEK spherulite at 320°C.

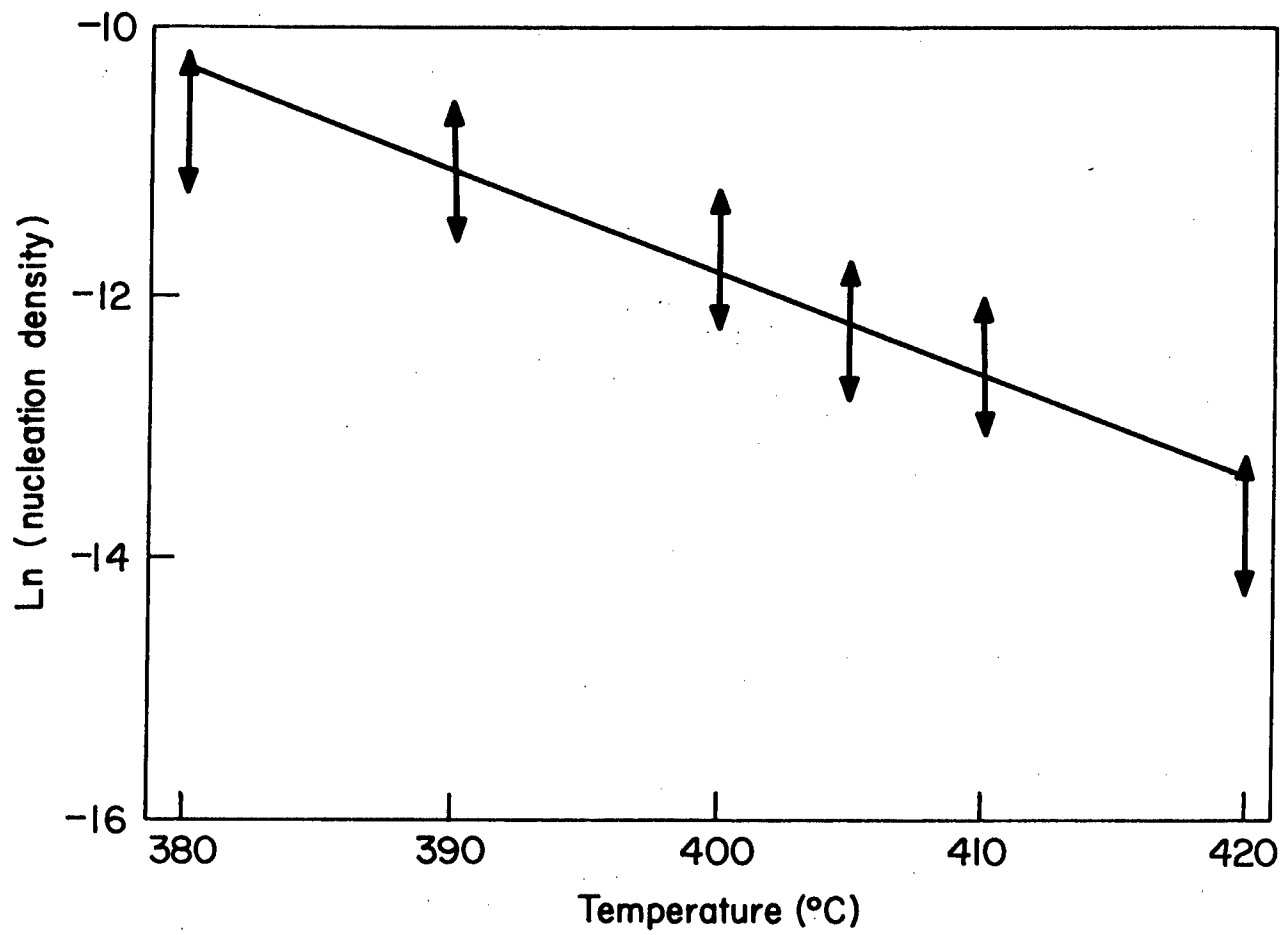


Figure 6. Plot of logarithm of nucleation density as a function of melt temperature.

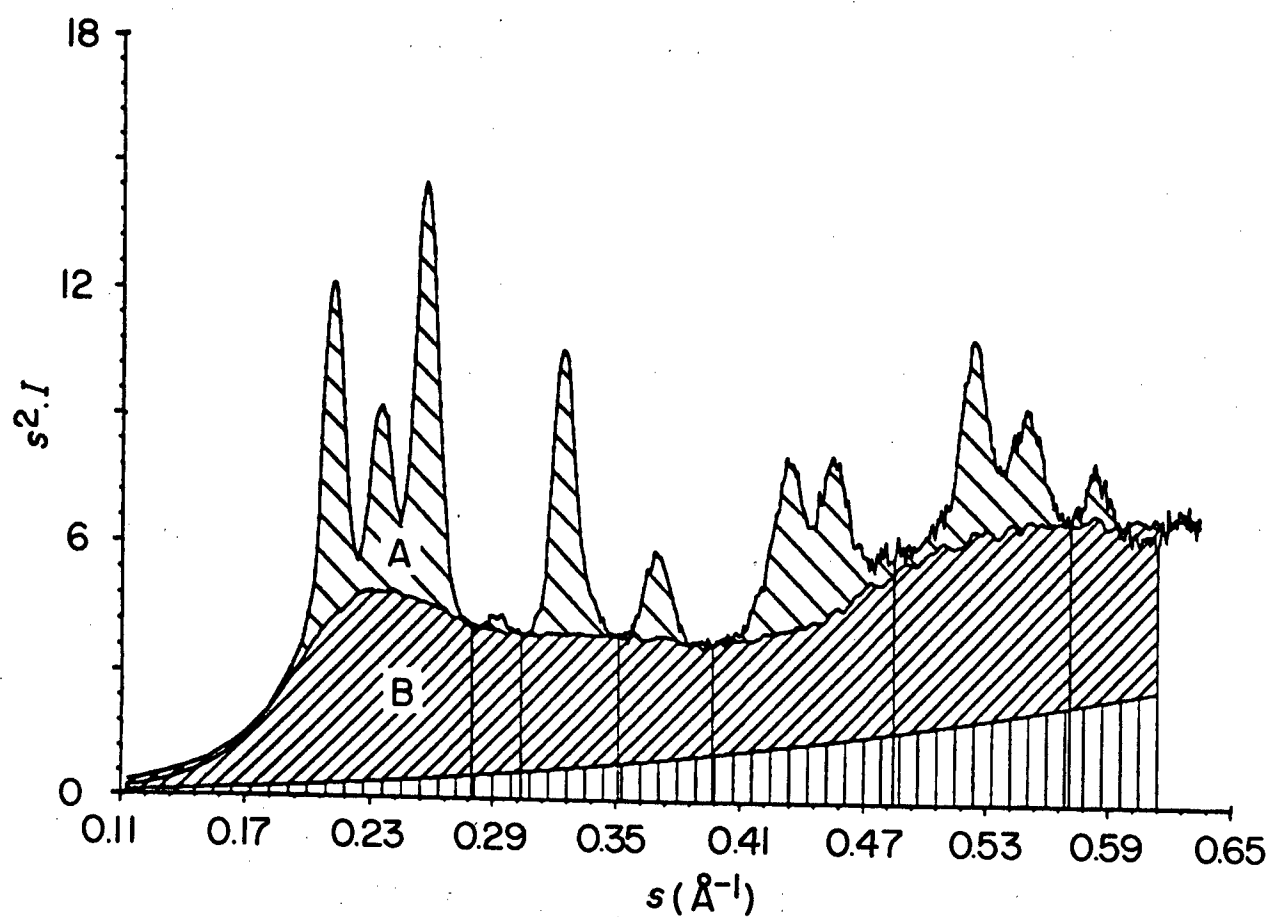


Figure 7. Typical WAXS curve of PEEK, curve-fitted using Pearson-VII-type function (ref. 24, 25). (A) crystalline, and (B) amorphous.

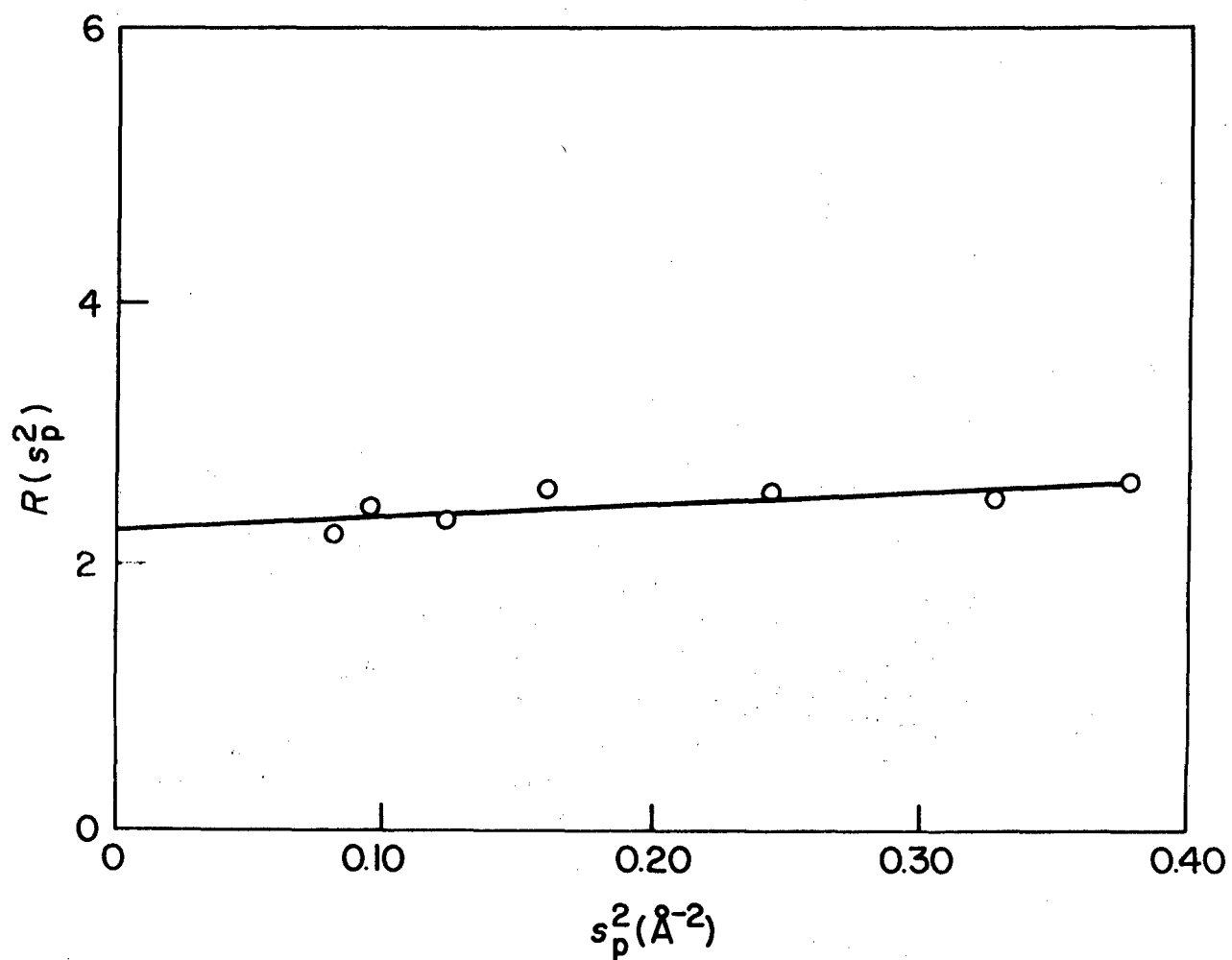


Figure 8. Vonk plot of $R(s_p)$ versus s_p .



Figure 9. Transmission electron micrograph (bright field) showing growth of spherulite. Regions marked "A" are amorphous and regions marked "B" are crystalline as determined from selected area electron diffraction.

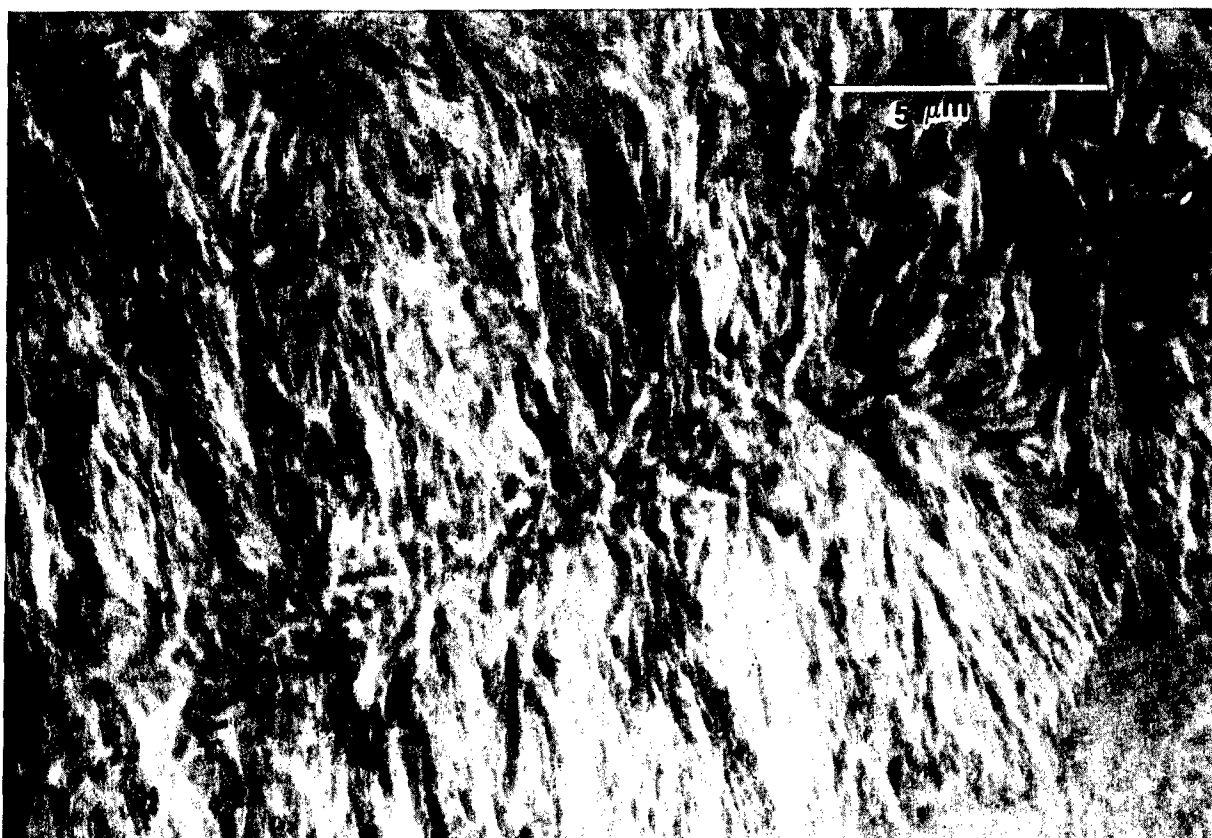


Figure 10. Row nucleation in PEEK as observed in transmission electron microscopy.

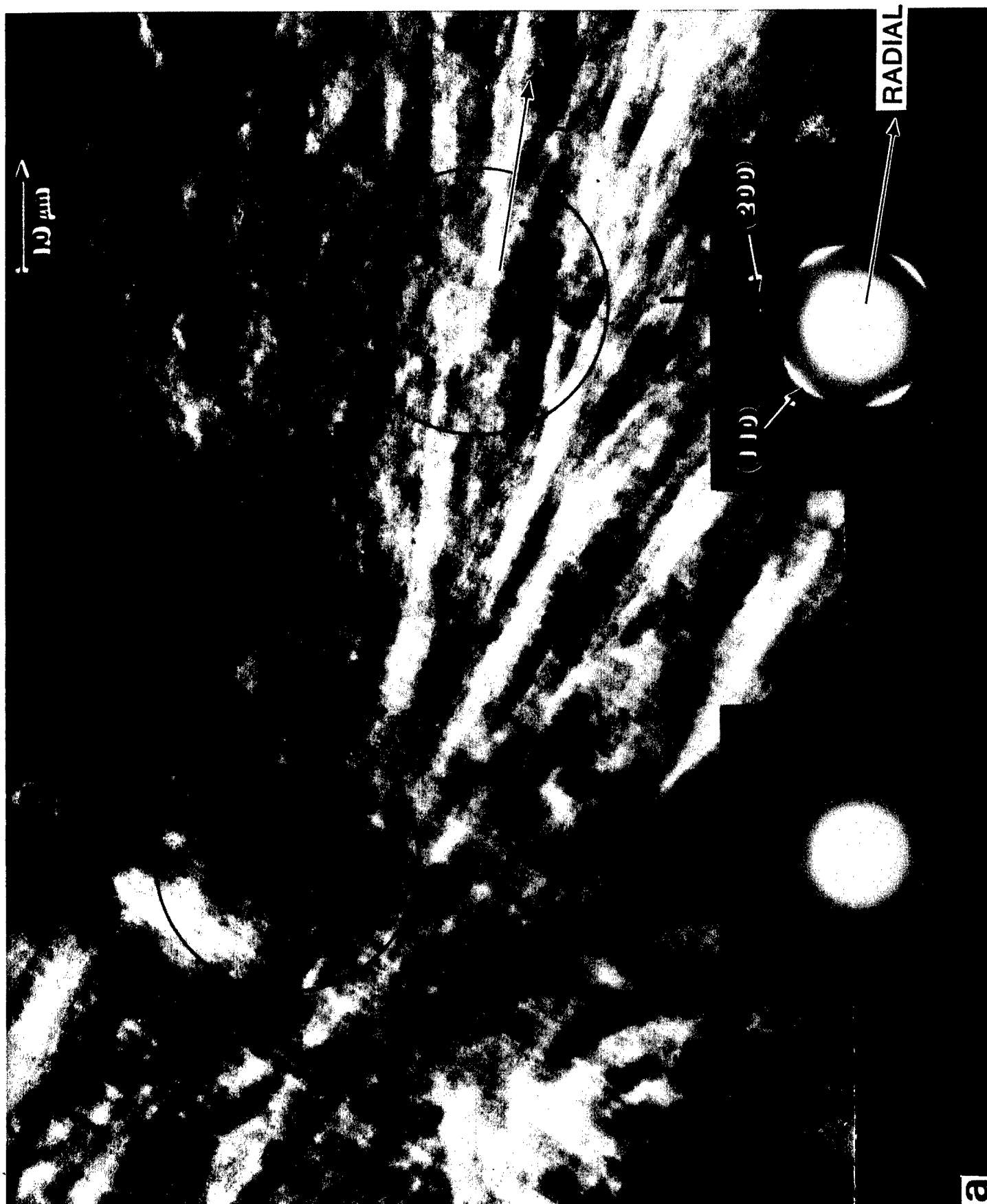


Figure 11.(a) Transmission electron micrographs (bright field) of spherulites seen along radius, (b) perpendicular to radius, and selected area electron diffraction patterns from the areas indicated with arrows.



Figure 11.(b) Figure 11 Concluded.

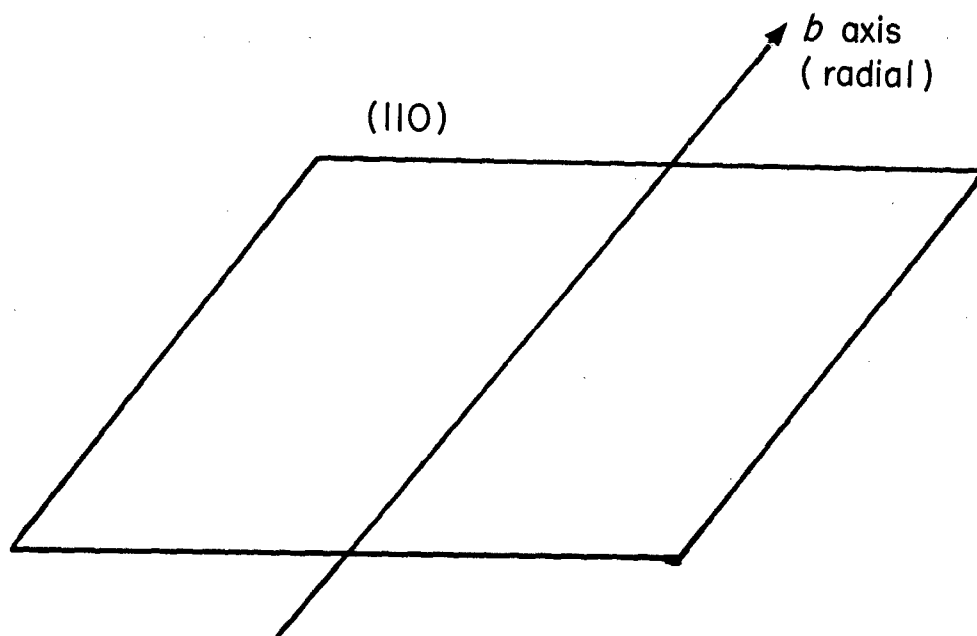


Figure 12. Transmission electron micrograph (dark field) using (110) plane and the schematic of crystal orientation.

TABLE 1
Bond polarizabilities of various bonds¹⁸⁻²⁰

Bond	α_1 (10^{-25} cm ³)	α_2 (10^{-25} cm ³)
C _{ar} - C _{ar}	22.5	4.8
C _{ar} - C _{al}	14.0	3.0
C - H	8.2	6.0
C - O	14.6	1.7
C = O	20.0	10.0

TABLE 2
PARAMETERS OBTAINED FROM WAXS AND SAXS

	Slow-cooled from 400 C	Slow-cooled from 420 C	Fast-cooled from 400 C
Degree of crystallinity	0.43	0.38	0.36
Disorder parameter	0.61	2.85	1.75
Crystal size (Å)			
from (211)	50	63	41
(110)	110	123	110
(200)	79	92	72
Long period (Å)	160	170	-
unit cell parameters (Å)			
a - axis	7.79	7.78	7.83
b - axis	5.91	5.90	5.92
c - axis	10.00	10.00	10.07